Commun. Comput. Phys.
doi: 10.4208/cicp.090313.041113a

Vol. **16**, No. 1, pp. 35-55
July 2014

Multi-Symplectic Fourier Pseudospectral Method for the Kawahara Equation

Yuezheng Gong, Jiaxiang Cai and Yushun Wang*

Jiangsu Key Laboratory for NSLSCS, School of Mathematical Sciences, Nanjing Normal University, Nanjing 210023, P.R. China.

Received 9 March 2013; Accepted (in revised version) 4 November 2013

Communicated by Lianjie Huang

Available online 28 March 2014

Abstract. In this paper, we derive a multi-symplectic Fourier pseudospectral scheme for the Kawahara equation with special attention to the relationship between the spectral differentiation matrix and discrete Fourier transform. The relationship is crucial for implementing the scheme efficiently. By using the relationship, we can apply the Fast Fourier transform to solve the Kawahara equation. The effectiveness of the proposed methods will be demonstrated by a number of numerical examples. The numerical results also confirm that the global energy and momentum are well preserved.

AMS subject classifications: 65M06, 65M70, 65T50, 65Z05, 70H15

Key words: Kawahara equation, Multi-symplecticity, Fourier pseudospectral method, FFT.

1 Introduction

In this paper, we consider the Kawahara equation [1]

$$2\frac{\partial u}{\partial t}+\alpha\frac{\partial^3 u}{\partial x^3}+\beta\frac{\partial^5 u}{\partial x^5}=\frac{\partial}{\partial x}f(u,u_x,u_{xx}), \tag{1.1}$$

where $u(x,t)$ is a scalar function, $\alpha,\beta\neq 0$ are real parameters and $f(u,u_x,u_{xx})$ is a smooth function. Eq. (1.1) is a model equation for plasma waves, capillary-gravity waves and other dispersive phenomena when the cubic KdV-type dispersion is weak. The form of (1.1) which occurs most often in applications is with $f(u,u_x,u_{xx})=au^2$, where a is a nonzero constant. Eq. (1.1) was first proposed by Kawahara [2] in 1972, as a model

*Corresponding author. *Email addresses:* `wangyushun@njnu.edu.cn` (Y. Wang), `gyz8814@aliyun.com` (Y. Gong), `thomasjeer@sohu.com` (J. Cai)

equation describing solitary-wave propagation in dispersive media. By studying systematically Eq. (1.1) with $f(u,u_x,u_{xx}) = -3u^2$, Kawahara observed that the solitary wave states could have oscillatory tails, and computed examples of such waves numerically. A more general nonlinearity was derived for water waves by Olver [3], using Hamiltonian perturbation theory, with further generalization given by Craig and Groves [4]. Existence and uniqueness of solutions to nonlinear Kawahara equations are obtained in [5].

As far as we know, numerical methods for this equation are very limited. Yuan, Shen and Wu [6] developed a Dual-Petrov-Galerkin method for the equation and showed some excellent numerical results. In Ref. [7], Hu and Deng developed a multi-symplectic Preissmann scheme. In this paper, we aim to develop a new multi-symplectic method for the Kawahara equation.

Many PDEs could be written as multi-symplectic Hamiltonian PDEs [8]

$$M\mathbf{z}_t + K\mathbf{z}_x = \nabla_{\mathbf{z}} S(\mathbf{z}), \tag{1.2}$$

where $\mathbf{z}(x,t) \in \mathbb{R}^n (n \geq 3)$, M and K are skew-symmetric matrices, and $S(\mathbf{z})$ is a smooth function. It is well known that Eq. (1.2) has multi-symplectic conservation law

$$\frac{\partial}{\partial t}\omega + \frac{\partial}{\partial x}\kappa = 0, \tag{1.3}$$

where $\omega = \frac{1}{2} d\mathbf{z} \wedge M d\mathbf{z}, \kappa = \frac{1}{2} d\mathbf{z} \wedge K d\mathbf{z}$. As the multi-symplectic conservation law is a signification geometric property of the Hamiltonian PDEs, numerical integrators which can preserve corresponding discrete multi-symplectic conservation law are expected. Bridges and Reich [9, 10] called such integrators are multi-symplectic integrators. Many equations were constructed as multi-symplectic Hamiltonian PDEs and integrated by some multi-symplectic methods (please refer to review paper [11]). These methods include multi-symplectic Preissmann scheme [9], multi-symplectic Fourier pseudospectral method [12, 13], multi-symplectic wavelet collocation method [14, 15], multi-symplectic Euler box scheme [16–19], multi-symplectic splitting method [20, 21] and so on. A great many numerical experiments show that multi-symplectic methods perform better than traditional numerical methods in long time simulations.

Bridges and Reich [12] suggested the idea of multi-symplectic spectral discretization on Fourier space. Based on their theory, Chen and Qin [13] proposed multi-symplectic Fourier pseudospectral (MSFP) method for Hamiltonian PDEs and applied it to integrate nonlinear Schrödinger (NLS) equation with periodic boundary conditions. Then, Wang [23] made some numerical analysis for the NLS equation. Later, the MSFP method was widely applied to other equations [14, 22, 24, 25] and so on. The key of the MSFP method is the spectral differentiation matrix (SDM) which can be obtained easily by proposed method in Ref. [13]. However, it needs a lot of storage space and a large amount of calculations to apply SDM directly, especially when the number of the nodes is large. In this paper, we develop a relationship between the SDM and discrete Fourier transform (DFT). By the relationship, we can apply Fast Fourier transform (FFT) easily in numerical calculation. To our knowledge, it has not been discussed that applying FFT to multi-symplectic scheme.

An outline of the paper is as follows. In Section 2, we review multi-symplectic structure for the Kawahara equation. In Section 3, we present the standard Fourier pseudospectral method and develop the relationship between the SDM and DFT. In Section 4, a MSFP method for the Kawahara equation is proposed by using Fourier pseudospectral method in space and midpoint implicit symplectic method in time. Numerical experiments are reported in Section 5. We finish the paper with conclusions in Section 6.

2 Multi-symplectic formulation of the Kawahara equation

In this section, we consider the Kawahara equation (1.1) with [1]

$$f(u,v,s)=F_u(u,v)-vF_{uv}(u,v)-sF_{vv}(u,v)+2sE_u(u,v)+svE_{uv}(u,v)+v^2E_{uu}(u,v).$$

Eq. (1.1) can be rewritten as the multi-symplectic Hamiltonian PDEs (1.2) with

$$\begin{aligned}
&\mathbf{z}=[\varphi,u,v,w,p,q]^T,\\
&S(\mathbf{z})=\frac{1}{2}\alpha v^2+\frac{1}{2\beta}q^2+wu+pv+F(u,v)+\frac{1}{2\beta}(2q+E(u,v))E(u,v),\\
&M=\begin{bmatrix} 0 & -1 & 0 & 0 & 0 & 0\\ 1 & 0 & 0 & 0 & 0 & 0\\ 0 & 0 & 0 & 0 & 0 & 0\\ 0 & 0 & 0 & 0 & 0 & 0\\ 0 & 0 & 0 & 0 & 0 & 0\\ 0 & 0 & 0 & 0 & 0 & 0 \end{bmatrix},\quad K=\begin{bmatrix} 0 & 0 & 0 & -1 & 0 & 0\\ 0 & 0 & 0 & 0 & -1 & 0\\ 0 & 0 & 0 & 0 & 0 & -1\\ 1 & 0 & 0 & 0 & 0 & 0\\ 0 & 1 & 0 & 0 & 0 & 0\\ 0 & 0 & 1 & 0 & 0 & 0 \end{bmatrix}.
\end{aligned}$$

It is well known that when $S(\mathbf{z})$ is independent of x and t then the multi-symplectic Hamiltonian PDEs (1.2) has a local energy conservation law

$$\mathcal{E}_t+\mathcal{F}_x=0 \quad \text{with} \quad \mathcal{E}(\mathbf{z})=S(\mathbf{z})-\frac{1}{2}\mathbf{z}^TK\mathbf{z}_x,\quad \mathcal{F}(\mathbf{z})=\frac{1}{2}\mathbf{z}^TK\mathbf{z}_t \tag{2.1}$$

and a local momentum conservation law

$$I_t+G_x=0 \quad \text{with} \quad G(\mathbf{z})=S(\mathbf{z})-\frac{1}{2}\mathbf{z}^TM\mathbf{z}_t,\quad I(\mathbf{z})=\frac{1}{2}\mathbf{z}^TM\mathbf{z}_x. \tag{2.2}$$

For the Kawahara equation, the corresponding local conservation laws (1.3)-(2.2) are given by

$$\begin{aligned}
&\omega=du\wedge d\varphi,\quad \kappa=dw\wedge d\varphi+dp\wedge du+dq\wedge dv,\\
&\mathcal{E}(\mathbf{z})=\frac{1}{2}\alpha v^2+F+\frac{1}{2\beta}(E^2-q^2),\quad \mathcal{F}(\mathbf{z})=w\varphi_t+pu_t+qv_t,\\
&G(\mathbf{z})=S(\mathbf{z})-u\varphi_t,\quad I(\mathbf{z})=u^2.
\end{aligned}$$

Under periodic boundary conditions, the above local conservation laws can be integrated in x-direction to obtain the global symplectic, energy and momentum conservation laws

$$\int \omega(x,t)dx = C_1, \quad \int \mathcal{E}(x,t)dx = C_2, \quad \int I(x,t)dx = C_3,$$

where C_1, C_2 and C_3 are constants which are independent of t.

3 The relationship between the SDM and DFT

Letting the spatial domain $I=[a,b]$ and $L=b-a$, we first consider Eq. (1.1) with the periodic boundary condition $u(x+L,t)=u(x,t)$ and recall Fourier pseudospectral method. Special attention is paid to the relationship between the SDM and DFT, which plays a crucial role in numerical computation.

The Fourier pseudospectral method involves two basic steps. First, we should construct the discrete representation of the solution through interpolate trigonometric polynomial of the solution at collocation points. Second, equations for the discrete values of the solution are obtained from the original equation. This second step involves finding an approximation for the differential operator in terms of the discrete values of the solution at collocation points.

We approximate $u(x,t)$ by $I_N u(x,t)$ which interpolate $u(x,t)$ at the following set of collocation points:

$$x_j = a + \frac{L}{N} j, \quad j = 0,1,\cdots,N-1,$$

where N is an even number. The approximation $I_N u(x,t)$ has the form

$$I_N u(x,t) = \sum_{n=0}^{N-1} u_n g_n(x), \tag{3.1}$$

where $u_n = u(x_n,t)$, $g_n(x_k) = \delta_n^k$. Therefore, we have

$$I_N u(x_j,t) = u_j, \quad j = 0,1,\cdots,N-1.$$

In fact, $g_n(x)$ can be given explicitly by

$$g_n(x) = \frac{1}{N} \sum_{l=-N/2}^{N/2} \frac{1}{c_l} e^{il\mu(x-x_n)}, \tag{3.2}$$

where $c_l = 1(|l| \neq N/2)$, $c_{-N/2} = c_{N/2} = 2$, $\mu = \frac{2\pi}{L}$. By directly computing, we can easily verify that $g_n(x_k) = \delta_n^k$.

The crucial step here is to obtain values for the derivative $\partial^k I_N u(x,t)/\partial x^k$ at the collocation points x_j in terms of the values u_j. We can do this by differentiating (3.1) and evaluating the resulting expressions at the points x_j:

$$\frac{\partial^k I_N u(x_j,t)}{\partial x^k} = \sum_{n=0}^{N-1} u_n \frac{d^k g_n(x_j)}{dx^k} = (D_k \mathbf{u})_j, \tag{3.3}$$

where D_k is an $N\times N$ matrix with elements

$$(D_k)_{j,n} = \frac{d^k g_n(x_j)}{dx^k}, \tag{3.4}$$

and $\mathbf{u}=[u_0,u_1,\cdots,u_{N-1}]^T$. We call D_k SDM. According to [13], we can obtain the following results explicitly

$$(D_1)_{j,n} = \begin{cases} \frac{1}{2}\mu(-1)^{j+n}\cot\Big(\mu\frac{x_j-x_n}{2}\Big), & j\neq n, \\ 0, & j=n, \end{cases} \tag{3.5}$$

$$(D_2)_{j,n} = \begin{cases} \frac{1}{2}\mu^2(-1)^{j+n+1}\frac{1}{\sin^2(\mu(x_j-x_n)/2)}, & j\neq n, \\ -\mu^2\frac{2(N/2)^2+1}{6}, & j=n. \end{cases} \tag{3.6}$$

Remark 3.1. If k is odd, D_k and D_1^k are real antisymmetric matrices; if k is even, D_k and D_1^k are real symmetric matrices. Moreover, if k is odd, $D_k = D_1^k$; if k is even, $D_k \neq D_1^k$ and $D_k = D_2^{\frac{k}{2}}$.

In order to study the property of the SDM, we reform (3.4) as follows

$$\begin{aligned}
(D_k)_{j,n} &= \frac{1}{N}\sum_{l=-N/2}^{N/2}\frac{(il\mu)^k}{c_l}e^{il\mu(x_j-x_n)} = \frac{1}{N}\sum_{l=-N/2}^{N/2}\frac{(il\mu)^k}{c_l}e^{i\frac{2\pi}{N}l(j-n)} = \frac{1}{N}\sum_{l=-N/2}^{N/2}\frac{(il\mu)^k}{c_l}W_N^{l(j-n)} \\
&= \frac{1}{N}\sum_{l=-N/2+1}^{N/2-1}(il\mu)^k W_N^{l(j-n)} + (-1)^{j+n}\frac{\mu^k}{2N}\Big[\Big(i\frac{N}{2}\Big)^k + \Big(-i\frac{N}{2}\Big)^k\Big] \\
&= \begin{cases} \frac{1}{N}\sum_{l=-N/2+1}^{N/2-1}(il\mu)^k W_N^{l(j-n)}, & k \text{ odd}, \\ \frac{1}{N}\sum_{l=-N/2+1}^{N/2}(il\mu)^k W_N^{l(j-n)}, & k \text{ even}, \end{cases} \\
&= \begin{cases} \frac{1}{N}\sum_{l=-N/2+1}^{N/2}(il\mu)^k W_N^{l(j-n)} - (-1)^{j+n}\frac{1}{N}\Big(i\frac{N}{2}\mu\Big)^k, & k \text{ odd}, \\ \frac{1}{N}\sum_{l=-N/2+1}^{N/2}(il\mu)^k W_N^{l(j-n)}, & k \text{ even}, \end{cases}
\end{aligned} \tag{3.7}$$

where $W_N = e^{i\frac{2\pi}{N}}$. Let

$$(A_k)_{j,n} = \frac{1}{N}\sum_{l=-N/2+1}^{N/2}(il\mu)^k W_N^{l(j-n)}, \qquad (B_k)_{j,n} = -(-1)^{j+n}\frac{1}{N}\left(i\frac{N}{2}\mu\right)^k, \tag{3.8}$$

we have

$$D_k = \begin{cases} A_k + B_k, & k \text{ odd}, \\ A_k, & k \text{ even}. \end{cases} \tag{3.9}$$

According to (3.8), we have followings very important conclusions.

Theorem 3.1. *Let*

$$m_l = \begin{cases} il\mu, & l = 0,1,\cdots,\dfrac{N}{2}, \\ i(l-N)\mu, & l = \dfrac{N}{2}+1,\cdots,N-1, \end{cases} \tag{3.10}$$

and $M = diag(m_0, m_1, \cdots, m_{N-1})$. Then we have

$$A_k = F^{-1}M^kF, \tag{3.11}$$

where F is discrete Fourier transform, and F^{-1} is discrete inverse Fourier transform.

Proof. First, we have from (3.8) and $W_N^{kN} = 1 (k \in \mathbb{Z})$

$$\begin{aligned}
(A_k)_{j,n} &= \frac{1}{N}\left[\sum_{l=0}^{N/2}(il\mu)^k W_N^{l(j-n)} + \sum_{l=-N/2+1}^{-1}(il\mu)^k W_N^{l(j-n)}\right] \\
&= \frac{1}{N}\left\{\sum_{l=0}^{N/2}(il\mu)^k W_N^{l(j-n)} + \sum_{l=N/2+1}^{N-1}[i(l-N)\mu]^k W_N^{(l-N)(j-n)}\right\} \\
&= \frac{1}{N}\left[\sum_{l=0}^{N/2} m_l^k W_N^{l(j-n)} + \sum_{l=N/2+1}^{N-1} m_l^k W_N^{l(j-n)}\right] \\
&= \frac{1}{N}\sum_{l=0}^{N-1} m_l^k W_N^{l(j-n)}.
\end{aligned}$$

Now we compute $F^{-1}M^kF$ directly. First,

$$F_{j,n} = W_N^{-jn}, \quad (F^{-1})_{j,n} = \frac{1}{N}W_N^{jn}, \quad M^k = diag(m_0^k, m_1^k, \cdots, m_{N-1}^k),$$

we have

$$\begin{aligned}
&(M^kF)_{j,n} = \sum_{l=0}^{N-1}(M^k)_{j,l}F_{l,n} = (M^k)_{j,j}F_{j,n} = m_j^k W_N^{-jn}, \\
&(F^{-1}M^kF)_{j,n} = \sum_{l=0}^{N-1}(F^{-1})_{j,l}(M^kF)_{l,n} = \sum_{l=0}^{N-1}\frac{1}{N}W_N^{jl}m_l^k W_N^{-ln} = \frac{1}{N}\sum_{l=0}^{N-1}m_l^k W_N^{l(j-n)}.
\end{aligned}$$

Hence, we obtain (3.11). $\square$

Theorem 3.2. *Let D_1 be defined by* (3.5)*, A_k and B_k be defined by* (3.8)*. Then we have*

$$D_1^k = A_k + B_k. \tag{3.12}$$

Proof. First, it follows from (3.7) that

$$(D_1)_{j,n} = \frac{1}{N} \sum_{l=-N/2+1}^{N/2-1} il\mu W_N^{l(j-n)}.$$

Now we compute $(D_1)^k$ directly. Note that

$$\frac{1}{N}\sum_{m=0}^{N-1} W_N^{lm} = \begin{cases} 0, & l \neq nN, \ n \text{ is an integer,} \\ 1, & l = nN, \end{cases}$$

we have

$$\begin{aligned}
(D_1^2)_{j,n} &= \sum_{m=0}^{N-1} (D_1)_{j,m}(D_1)_{m,n} \\
&= \sum_{m=0}^{N-1} \left(\frac{1}{N} \sum_{l=-N/2+1}^{N/2-1} il\mu W_N^{l(j-m)} \right) \left(\frac{1}{N} \sum_{p=-N/2+1}^{N/2-1} ip\mu W_N^{p(m-n)} \right) \\
&= \frac{1}{N} \sum_{l=-N/2+1}^{N/2-1} \sum_{p=-N/2+1}^{N/2-1} (il\mu)(ip\mu) W_N^{lj-pn} \left(\frac{1}{N} \sum_{m=0}^{N-1} W_N^{m(p-l)} \right) \\
&= \frac{1}{N} \sum_{l=-N/2+1}^{N/2-1} (il\mu)^2 W_N^{l(j-n)}.
\end{aligned}$$

Similarly, we have

$$\begin{aligned}
(D_1^3)_{j,n} &= \sum_{m=0}^{N-1} (D_1^2)_{j,m}(D_1)_{m,n} \\
&= \sum_{m=0}^{N-1} \left(\frac{1}{N} \sum_{l=-N/2+1}^{N/2-1} (il\mu)^2 W_N^{l(j-m)} \right) \left(\frac{1}{N} \sum_{p=-N/2+1}^{N/2-1} ip\mu W_N^{p(m-n)} \right) \\
&= \frac{1}{N} \sum_{l=-N/2+1}^{N/2-1} \sum_{p=-N/2+1}^{N/2-1} (il\mu)^2(ip\mu) W_N^{lj-pn} \left(\frac{1}{N} \sum_{m=0}^{N-1} W_N^{m(p-l)} \right) \\
&= \frac{1}{N} \sum_{l=-N/2+1}^{N/2-1} (il\mu)^3 W_N^{l(j-n)}.
\end{aligned}$$

Applying induction on k leads to

$$(D_1^k)_{j,n} = \frac{1}{N} \sum_{l=-N/2+1}^{N/2-1} (il\mu)^k W_N^{l(j-n)}.$$

Hence, we obtain

$$
\begin{aligned}
(D_1^k)_{j,n} &= \frac{1}{N}\sum_{l=-N/2+1}^{N/2} (il\mu)^k W_N^{l(j-n)} - (-1)^{j+n}\frac{1}{N}\Big(i\frac{N}{2}\mu\Big)^k \\
&= (A_k)_{j,n} + (B_k)_{j,n}.
\end{aligned}
$$

This verifies (3.12). □

Remark 3.2. 1. We note that

$$
B_k = -\frac{1}{N}\Big(i\frac{N}{2}\mu\Big)^k bb^T, \tag{3.13}
$$

where $b=[1,-1,\cdots,1,-1]^T\in\mathbb{R}^N$.

2. By the relation (3.11) and (3.12), we can evaluate the derivatives by using the FFT algorithm instead of spectral differentiation matrix in $\mathcal{O}(N\log N)$ operations rather than $\mathcal{O}(N^2)$ operations.

4 The MSFP method for the Kawahara equation

In this section, we derive the multi-symplectic structure of the Fourier pseudospectral method for the Kawahara equation. We can rewrite the multi-symplectic formulation of Eq. (1.1) as

$$
\begin{cases}
-u_t - w_x = 0, \\
\varphi_t - p_x = w + F_u + \dfrac{1}{\beta}(q+E)E_u, \\
-q_x = \alpha v + p + F_v + \dfrac{1}{\beta}(q+E)E_v, \\
\varphi_x = u, \qquad u_x = v, \\
v_x = \dfrac{1}{\beta}(q+E).
\end{cases} \tag{4.1}
$$

Applying the Fourier pseudospectral method in space to the multi-symplectic system (4.1) and using the notations

$$
\begin{aligned}
&U=[u_0,u_1,\cdots,u_{N-1}]^T, \quad V=[v_0,v_1,\cdots,v_{N-1}]^T, \quad W=[w_0,w_1,\cdots,w_{N-1}]^T, \\
&P=[p_0,p_1,\cdots,p_{N-1}]^T, \quad Q=[q_0,q_1,\cdots,q_{N-1}]^T, \quad \Phi=[\varphi_0,\varphi_1,\cdots,\varphi_{N-1}]^T, \\
&E(U,V)=[E(u_0,v_0),\ E(u_1,v_1),\cdots,E(u_{N-1},v_{N-1})]^T, \\
&UV=[u_0v_0,\ u_1v_1,\cdots,u_{N-1}v_{N-1}]^T,
\end{aligned}
$$

we can get a semi-discrete system of (4.1)

$$\begin{cases} -\dfrac{du_j}{dt}-(D_1W)_j=0, \\ \dfrac{d\varphi_j}{dt}-(D_1P)_j=w_j+F_u(u_j,v_j)+\dfrac{1}{\beta}(q_j+E(u_j,v_j))E_u(u_j,v_j), \\ -(D_1Q)_j=\alpha v_j+p_j+F_v(u_j,v_j)+\dfrac{1}{\beta}(q_j+E(u_j,v_j))E_v(u_j,v_j), \\ (D_1\Phi)_j=u_j, \qquad (D_1U)_j=v_j, \\ (D_1V)_j=\dfrac{1}{\beta}(q_j+E(u_j,v_j)). \end{cases} \tag{4.2}$$

Theorem 4.1. *The Fourier pseudospectral semi-discretization* (4.2) *has N semi-discrete multi-symplectic conservation laws*

$$\frac{d}{dt}\omega_j+\sum_{k=0}^{N-1}(D_1)_{j,k}\kappa_{j,k}=0, \quad j=0,1,\cdots,N-1, \tag{4.3}$$

where $\omega_j=\frac{1}{2}d\mathbf{z}_j\wedge Md\mathbf{z}_j$, $\kappa_{j,k}=d\mathbf{z}_j\wedge Kd\mathbf{z}_k$.

Proof. We rewrite (4.2) in the compact form

$$M\frac{d}{dt}\mathbf{z}_j+K\sum_{k=0}^{N-1}(D_1)_{j,k}\mathbf{z}_k=\nabla_{\mathbf{z}}S(\mathbf{z}_j). \tag{4.4}$$

The variational equation associated with (4.4) is

$$M\frac{d}{dt}d\mathbf{z}_j+K\sum_{k=0}^{N-1}(D_1)_{j,k}d\mathbf{z}_k=S_{\mathbf{zz}}(\mathbf{z}_j)d\mathbf{z}_j. \tag{4.5}$$

Taking the wedge product with $d\mathbf{z}_j$ and noting the fact

$$d\mathbf{z}_j\wedge S_{\mathbf{zz}}(\mathbf{z}_j)d\mathbf{z}_j=0, \quad d\mathbf{z}_j\wedge Md\mathbf{z}_k=d\mathbf{z}_k\wedge Md\mathbf{z}_j,$$

we obtain the N multi-symplectic conservation laws (4.3). □

Since D_1 is antisymmetric and $\kappa_{jk}=\kappa_{kj}$, we can sum (4.3) over the spatial index, and then obtain

$$\frac{d}{dt}\sum_{j=0}^{N-1}\omega_j=0, \tag{4.6}$$

which implies conservation of the total symplecticity over time [12]. Thus it is natural to integrate with respect to time using a symplectic integrator. Applying the midpoint symplectic integration in time, we obtain the MSFP method for Eq. (1.1)

$$\begin{cases} -D_t u_j^n - (A_t D_1 W^n)_j = 0, \\ D_t \varphi_j^n - (A_t D_1 P^n)_j = A_t w_j^n + F_u(A_t u_j^n, A_t v_j^n) \\ \qquad\qquad + \dfrac{1}{\beta}(A_t q_j^n + E(A_t u_j^n, A_t v_j^n)) E_u(A_t u_j^n, A_t v_j^n), \\ -(A_t D_1 Q^n)_j = \alpha A_t v_j^n + A_t p_j^n + F_v(A_t u_j^n, A_t v_j^n) \\ \qquad\qquad + \dfrac{1}{\beta}(A_t q_j^n + E(A_t u_j^n, A_t v_j^n)) E_v(A_t u_j^n, A_t v_j^n), \\ (A_t D_1 \Phi^n)_j = A_t u_j^n, \qquad (A_t D_1 U^n)_j = A_t v_j^n, \\ (A_t D_1 V^n)_j = \dfrac{1}{\beta}(A_t q_j^n + E(A_t u_j^n, A_t v_j^n)), \end{cases} \tag{4.7}$$

where $D_t u_j^n = (u_j^{n+1} - u_j^n)/\Delta t$ and $A_t u_j^n = (u_j^{n+1} + u_j^n)/2$.

Theorem 4.2. *The scheme* (4.7) *has N full-discrete multi-symplectic conservation laws*

$$\frac{\omega_j^{n+1} - \omega_j^n}{\Delta t} + \sum_{k=0}^{N-1} (D_1)_{j,k} \kappa_{j,k}^{n+1/2} = 0, \quad j = 0,1,\cdots,N-1, \tag{4.8}$$

where $\omega_j^n = \frac{1}{2} d\mathbf{z}_j^n \wedge M d\mathbf{z}_j^n$, $\kappa_{j,k}^{n+1/2} = d\mathbf{z}_j^{n+1/2} \wedge K d\mathbf{z}_k^{n+1/2}$, $\mathbf{z}_k^{n+1/2} = (\mathbf{z}_k^{n+1} + \mathbf{z}_k^n)/2$.

Proof. From Theorem 4.1, we know that (4.7) can be rewritten in the compact form

$$M \frac{\mathbf{z}_j^{n+1} - \mathbf{z}_j^n}{\Delta t} + K \sum_{k=0}^{N-1} (D_1)_{j,k} \mathbf{z}_k^{n+1/2} = \nabla_{\mathbf{z}} S(\mathbf{z}_j^{n+1/2}). \tag{4.9}$$

The variational equation associated with (4.9) is

$$M \frac{d\mathbf{z}_j^{n+1} - d\mathbf{z}_j^n}{\Delta t} + K \sum_{k=0}^{N-1} (D_1)_{j,k} d\mathbf{z}_k^{n+1/2} = S_{\mathbf{zz}}(\mathbf{z}_j^{n+1/2}) d\mathbf{z}_j^{n+1/2}. \tag{4.10}$$

Taking the wedge product with $d\mathbf{z}_j^{n+1/2}$ and noting the fact

$$d\mathbf{z}_j^{n+1/2} \wedge S_{\mathbf{zz}}(\mathbf{z}_j^{n+1/2}) d\mathbf{z}_j^{n+1/2} = 0, \quad d\mathbf{z}_j^{n+1/2} \wedge M d\mathbf{z}_k^{n+1/2} = d\mathbf{z}_k^{n+1/2} \wedge M d\mathbf{z}_j^{n+1/2},$$

we obtain the full-discrete multi-symplectic conservation laws (4.8). □

Since D_1 is antisymmetric and $\kappa_{jk}^{n+1/2} = \kappa_{kj}^{n+1/2}$, summing (4.8) over the spatial index gives

$$\sum_{j=0}^{N-1} \omega_j^{n+1} = \sum_{j=0}^{N-1} \omega_j^n. \tag{4.11}$$

The system (4.7) can be written into a vector form

$$\begin{cases} D_tU^n + A_tD_1W^n = 0, \\ D_t\Phi^n - A_tD_1P^n = A_tW^n + F_u(A_tU^n, A_tV^n) \\ \qquad\qquad\qquad + \dfrac{1}{\beta}(A_tQ^n + E(A_tU^n, A_tV^n))E_u(A_tU^n, A_tV^n), \\ -D_1A_tQ^n = \alpha A_tV^n + A_tP^n + F_v(A_tU^n, A_tV^n) \\ \qquad\qquad\qquad + \dfrac{1}{\beta}(A_tQ^n + E(A_tU^n, A_tV^n))E_v(A_tU^n, A_tV^n), \\ A_tD_1\Phi^n = A_tU^n, \quad A_tD_1U^n = A_tV^n, \\ A_tD_1V^n = \dfrac{1}{\beta}(A_tQ^n + E(A_tU^n, A_tV^n)). \end{cases} \tag{4.12}$$

Further, eliminating the auxiliary variables φ, v, w, p, q in Eq. (4.12), we obtain an equivalent scheme

$$\begin{aligned} &2A_tD_tU^n + \alpha A_t^2D_1^3U^n + \beta A_t^2D_1^5U^n \\ =& A_tD_1(F_u(A_tU^n, A_tV^n) + (A_tD_1^2U^n)E_u(A_tU^n, A_tV^n)) + A_tD_1^3E(A_tU^n, A_tV^n) \\ &- A_tD_1^2F_v(A_tU^n, A_tV^n) - A_tD_1^2((A_tD_1^2U^n)E_v(A_tU^n, A_tV^n)). \end{aligned} \tag{4.13}$$

Then we give a two time levels scheme for (1.1)

$$\begin{aligned} &2D_tU^n + \alpha A_tD_1^3U^n + \beta A_tD_1^5U^n \\ =& D_1(F_u(A_tU^n, A_tV^n) + (A_tD_1^2U^n)E_u(A_tU^n, A_tV^n)) + D_1^3E(A_tU^n, A_tV^n) \\ &- D_1^2F_v(A_tU^n, A_tV^n) - D_1^2((A_tD_1^2U^n)E_v(A_tU^n, A_tV^n)). \end{aligned} \tag{4.14}$$

In the numerical experiments, we can use the two time levels scheme (4.14) to give the initial datum for the second level values of the three time levels scheme (4.13). In order to apply FFT to solve scheme (4.13), we would use the relationship $D_1^k = A_k + B_k$ (see Section 3).

5 Numerical results

In this section, we present some numerical results for the Kawahara and modified Kawahara equations.

5.1 Solitary waves

We consider first the Kawahara equation [6]

$$u_t + uu_x + u_{xxx} - u_{xxxxx} = 0, \quad u(x,0) = u_{ex}(x,0), \tag{5.1}$$

where

$$u_{ex}(x,t)=\frac{105}{169}\text{sech}^4\Big(\frac{1}{2\sqrt{13}}\Big(x-\frac{36t}{169}-x_0\Big)\Big) \tag{5.2}$$

is an exact soliton solution of (5.1); and the modified Kawahara equation

$$u_t+u_x+u^2u_x+pu_{xxx}+qu_{xxxxx}=0, \quad u(x,0)=u_{ex}(x,0), \tag{5.3}$$

where

$$u_{ex}(x,t)=\pm\frac{3p}{\sqrt{-10q}}\text{sech}^2\Big(\frac{1}{2}\sqrt{\frac{-p}{5q}}\Big(x-\frac{25q-4p^2}{25q}t-x_0\Big)\Big) \tag{5.4}$$

is an exact soliton solution of (5.3) and p, q are two parameters.

We fix $x_0=0$ and restrict the problem to the finite interval $[-L,L]$ with L sufficiently large such that the solution $u_{ex}(\pm L,t)$, $\partial_x u_{ex}(\pm L,t)$, $\partial_x^2 u_{ex}(L,t)$ are essentially zero for $t\in[0,T]$ (where T is given). We apply the scaling $\widetilde{x}=L^{-1}x$, $\widetilde{t}=L^{-1}t$, and for the sake of simplicity, still use (x,t) to denote $(\widetilde{x},\widetilde{t})$. Then we are led to consider the following scaled Kawahara equation

$$u_t+uu_x+\frac{1}{L^2}u_{xxx}-\frac{1}{L^4}u_{xxxxx}=0, \quad x\in(-1,1), \tag{5.5a}$$

$$u(\pm1)=u_x(\pm1)=u_{xx}(1)=0, \tag{5.5b}$$

$$u(x,0)=\frac{105}{169}\text{sech}^4\Big(\frac{L}{2\sqrt{13}}x\Big), \tag{5.5c}$$

and the modified Kawahara equation

$$u_t+u_x+u^2u_x+\frac{1}{L^2}u_{xxx}-\frac{1}{L^4}u_{xxxxx}=0, \quad x\in(-1,1), \tag{5.6a}$$

$$u(\pm1)=u_x(\pm1)=u_{xx}(1)=0, \tag{5.6b}$$

$$u(x,0)=\frac{3}{\sqrt{10}}\text{sech}^2\Big(\frac{L}{2\sqrt{5}}x\Big). \tag{5.6c}$$

5.1.1 The Kawahara equation

For Eq. (5.5), we fix the parameters $L=200$, $\alpha=\frac{2}{L^2}$, $\beta=-\frac{2}{L^4}$, and the function $E=0$, $F=-u^3/3$.

We choose $T=1$ and $\triangle t=1.0E-4$. The error due to spatial discretization decreases quickly as the number of grid points N is increased, but the error will not decrease after a critical value of N (see Table 1). If we instead keep $N=256$ and $N=1024$ fixed, respectively, and decrease the time step, we get the result shown in Tables 2 and 3. Table 2 $(N=256)$ shows that the convergence rate declines with the decrease of time step. Note that in Table 3, the spatial error $(N=1024)$ is negligible and the error is dominated by the time discretization error. Table 3 clearly indicates that the midpoint implicit symplectic scheme is of second-order in time. Next, we make some comparison with the method

Table 1: The error due to spatial discretization decreases quickly as the number of grid points N is increased ($T=1$, $\triangle t=1.0E-4$).

N	L^∞-error	Ratio
128	7.5877e-003	
256	7.3931e-007	10263
512	7.7065e-007	0.9593
1024	7.7065e-007	1.0000
2048	7.7067e-007	1.0000

Table 2: The error due to temporal discretization decreases as time step $\triangle t$ is decreased ($T=1$, $N=256$).

$\triangle t$	L^2-error	Ratio
0.001	1.6189e-005	
$2^{-1}\cdot 0.001$	4.0474e-006	3.9999
$2^{-2}\cdot 0.001$	1.0121e-006	3.9990
$2^{-3}\cdot 0.001$	2.5402e-007	3.9843
$2^{-4}\cdot 0.001$	6.7677e-008	3.7534
$2^{-5}\cdot 0.001$	2.9005e-008	2.3333

Table 3: The error due to temporal discretization decreases as time step $\triangle t$ is decreased ($T=1$, $N=1024$).

$\triangle t$	L^2-error	Ratio
0.001	1.6189e-005	
$2^{-1}\cdot 0.001$	4.0474e-006	3.9999
$2^{-2}\cdot 0.001$	1.0119e-006	3.9998
$2^{-3}\cdot 0.001$	2.5296e-007	4.0002
$2^{-4}\cdot 0.001$	6.3241e-008	3.9999
$2^{-5}\cdot 0.001$	1.5810e-008	4.0001

Table 4: L^2-error for solitary wave solutions in the Kawahara equation (Ref. [6]).

Time	$\triangle t=1.0E-4$	$\triangle t=2.0E-4$	Ratio
0.5	3.44E-7	1.374E-6	3.99
1.0	5.926E-7	2.358E-6	3.98
2.0	1.104E-6	4.389E-6	3.98
4.0	2.147E-6	8.494E-6	3.96

in [6]. The results are displayed in Tables 4 and 5. One can see that the results obtained by our method are better than those of method in Ref. [6].

In order to further testing the proposed method, we solve Eq. (5.5) for $t\in(0,10)$ (which corresponds to the real time $t\in(0,2000)$). Fig. 1 shows the variation of the solution errors obtained with $N=256$ ($N=1024$) and $\triangle t=1.0E-4$. We note that solitary waves of the Kawahara equation have shape stability but not phase stability [26]. Because a phase drift is linear in t, the numerical errors look like to show linear growth.

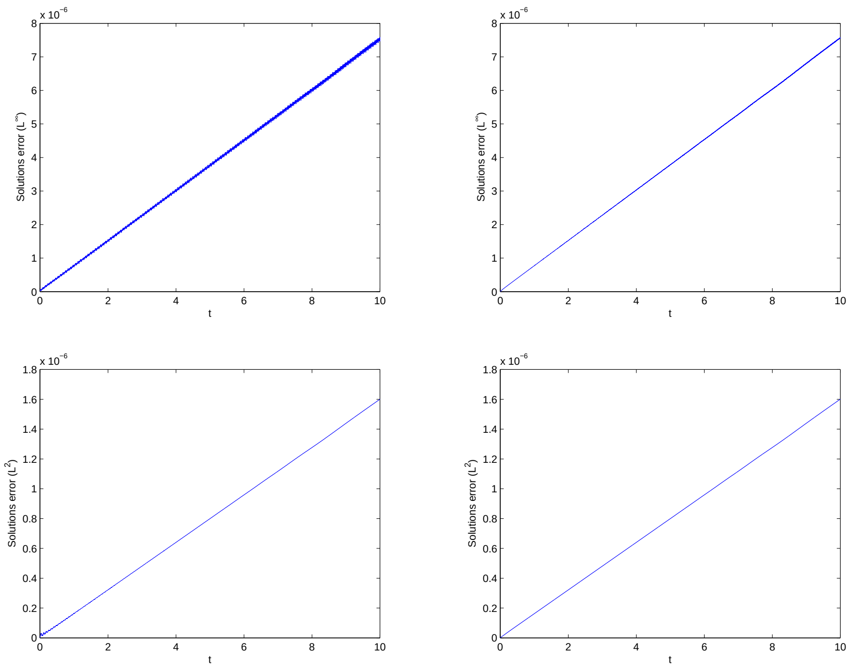

Figure 1: For the Kawahara equation, maximum solution errors L^∞ (upper) and average solution errors L^2 (lower) with $N=256$ (left) and $N=1024$ (right) ($\triangle t=1.0E-4$).

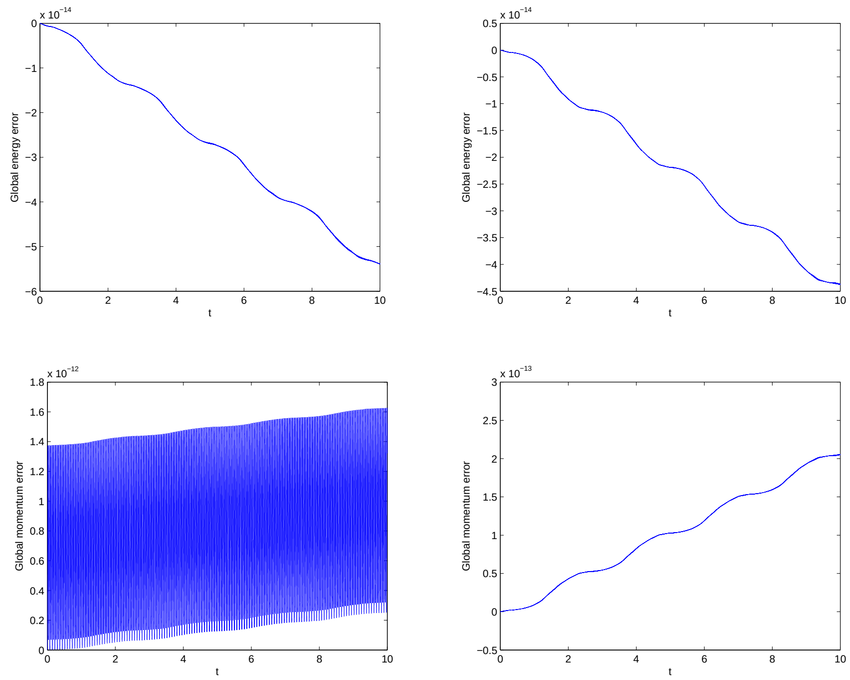

Figure 2: For the Kawahara equation, global energy errors (upper) and global momentum errors (lower) with $N=256$ (left) and $N=1024$ (right) ($\triangle t=1.0E-4$).

Table 5: L^2-error for solitary wave solutions in the Kawahara equation ($N=1000$).

Time	$\triangle t=1.0E-4$	$\triangle t=2.0E-4$	Ratio
0.5	8.2236e-008	3.2894e-007	4.0000
1.0	1.6190e-007	6.4759e-007	3.9999
2.0	3.2117e-007	1.2847e-006	4.0001
4.0	6.3981e-007	2.5592e-006	3.9999

Now, we display the energy and momentum preservation of the proposed scheme. Eqs. (5.5) and (5.6) with periodic boundary condition have global energy and momentum conservation law

$$\int \mathcal{E}(x,t)dx=C_2, \quad \mathcal{E}=\frac{\alpha}{2}u_x^2-\frac{\beta}{2}u_{xx}^2+F$$

and global momentum conservation law

$$\int I(x,t)dx=C_3, \quad I=u^2.$$

Define the errors in discrete global energy and momentum as

$$GE=\sum_{j=0}^{N-1}(\mathcal{E}_j^n-\mathcal{E}_j^0)\Delta x \quad \text{and} \quad GI=\sum_{j=0}^{N-1}(I_j^n-I_j^0)\Delta x,$$

where

$$\mathcal{E}_j^n=\frac{\alpha}{2}(D_1U^n)_j^2-\frac{\beta}{2}(D_1^2U^n)_j^2+F_j^n \quad \text{and} \quad I_j^n=(u_j^n)^2.$$

In Fig. 2, we present the errors in discrete global energy and momentum. From these graphs, we also see that the numerical errors look like to show linear growth. Nevertheless, global energy and momentum are preserved well.

5.1.2 The modified Kawahara equation

For Eq. (5.6), we fix the parameters $L=200$, $\alpha=\frac{2}{L^2}$, $\beta=-\frac{2}{L^4}$, and the function $E=0$, $F=-u^2-\frac{1}{6}u^4$. Similarly, we make comparison with the method in [6]. We can get the same conclusions as Subsection 5.1.1 (see Tables 6,7 and Figs. 3,4).

5.2 Oscillatory solitary waves

We now consider the following Kawahara equation [6]

$$u_t-6uu_x-u_{xxx}-u_{xxxxx}=0, \tag{5.7}$$

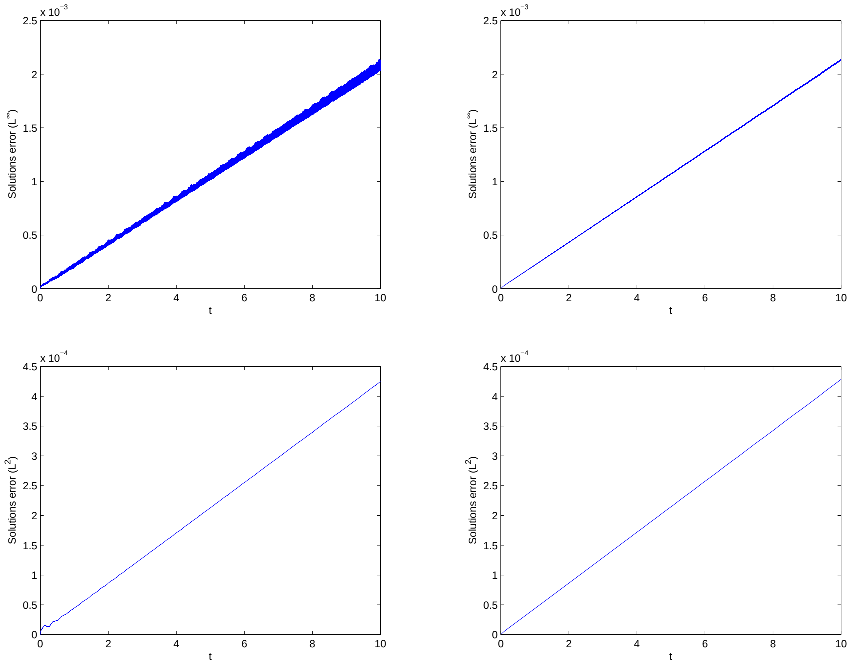

Figure 3: For the modified Kawahara equation, maximum solution errors L^{∞} (upper) and average solution errors L^{2} (lower) with $N=256$ (left) and $N=1024$ (right) ($\triangle t=1.0E-4$).

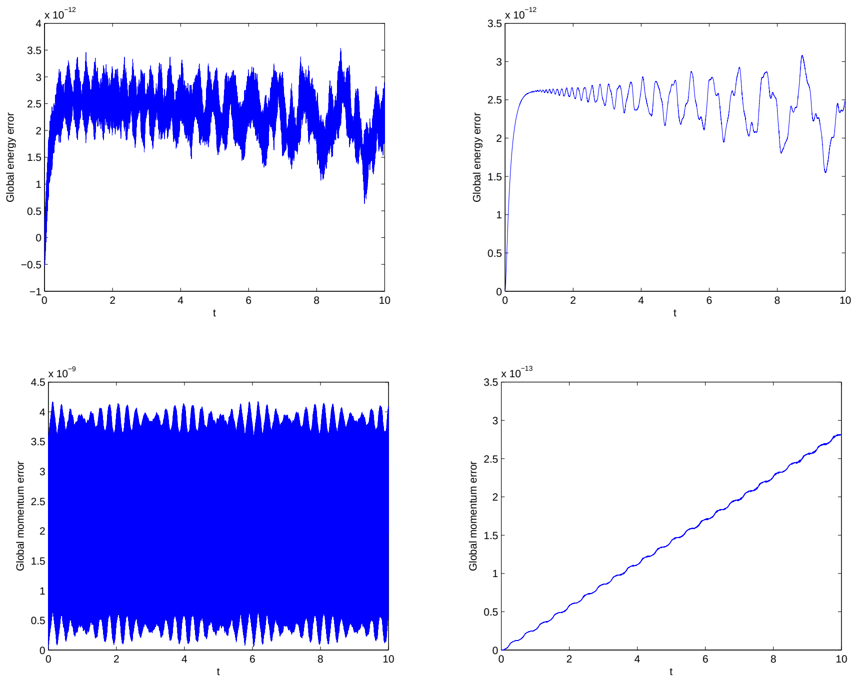

Figure 4: For the modified Kawahara equation, global energy errors (upper) and global momentum errors (lower) with $N=256$ (left) and $N=1024$ (right) ($\triangle t=1.0E-4$).

Table 6: L^2-error for solitary wave solutions in the modified Kawahara equation (Ref. [6]).

Time	$\triangle t = 1.0E-4$	$\triangle t = 2.0E-4$	Ratio
0.1	1.77E-5	7.071E-5	4
0.2	2.93E-5	1.173E-4	4
0.4	5.19E-5	2.076E-4	4
0.5	6.33E-5	2.531E-4	4

Table 7: L^2-error for solitary wave solutions in the modified Kawahara equation ($N=1000$).

Time	$\triangle t = 1.0E-4$	$\triangle t = 2.0E-4$	Ratio
0.1	5.3255e-006	2.1300e-005	3.9996
0.2	9.7775e-006	3.9106e-005	3.9996
0.4	1.8279e-005	7.3106e-005	3.9995
0.5	2.2506e-005	9.0011e-005	3.9994

which has the following asymptotic solution

$$\begin{aligned} u_{ex}(x,t) = \sqrt{\frac{2}{19}}\epsilon\cos\theta\,\text{sech}\, X + \epsilon^2 \Big\{ & \frac{187}{57\sqrt{19}}\sin\theta\,\text{sech}\, X \tanh X \\ & - \frac{4}{19}\Big(3+\frac{1}{3}\cos 2\theta\Big)\text{sech}^{\,2} X \Big\} + \mathcal{O}(\epsilon^3) := \bar{u}(x,t) + \mathcal{O}(\epsilon^3), \end{aligned} \tag{5.8}$$

where $\theta = \sqrt{0.5}(x-0.25t)$, $X = \epsilon(x-0.25t)$, $0<\epsilon \ll 1$.

We rescale (5.7) with $(\widetilde{x},\widetilde{t}) = (L^{-1}x, L^{-1}t)$, still use (x,t) to denote $(\widetilde{x},\widetilde{t})$, we are led to consider the following initial- and boundary-value problem:

$$u_t - 6uu_x - \frac{1}{L^2}u_{xxx} - \frac{1}{L^4}u_{xxxxx} = 0, \tag{5.9a}$$

$$u(\pm 1,t) = u_x(\pm 1,t) = u_{xx}(1,t) = 0, \tag{5.9b}$$

$$u(x,0) = \bar{u}(Lx,0). \tag{5.9c}$$

In our numerical experiments, we take $\epsilon = 0.01$, $L = 2000$, $\alpha = -\frac{2}{L^2}$, $\beta = -\frac{2}{L^4}$, and the function $E=0$, $F=2u^3$. Note that for smaller ϵ, larger L is needed to ensure that the boundary conditions in (5.9) are sufficiently accurate. In all the computations presented below, we use $\Delta t = 1.0E-5$ and $N=2000$. In Table 8, we list the L^2 and L^∞ errors between the computed solutions of (5.9) and the asymptotic solution at three different (scaled) times $t = 0.05$, 0.1, 0.2 which correspond to original times $t = 100$, 200, 400. Note that the accuracy is limited by the accuracy of the asymptotic solution which is accurate to the order of ϵ^3.

In Figs. 5-10, we plot the computed solutions and the asymptotic solutions at three different times on the whole interval (Figs. 5, 7 and 9) and on a shorter interval (Figs. 6,

Table 8: Differences between the computed solutions of (5.9) and the asymptotic solution with $\epsilon = 0.01$ and $\Delta t = 1.0E-5$.

t	L^2	L^∞
0.05	1.0249e-005	4.5470e-005
0.1	2.0497e-005	9.0700e-005
0.2	4.0991e-005	1.8187e-004

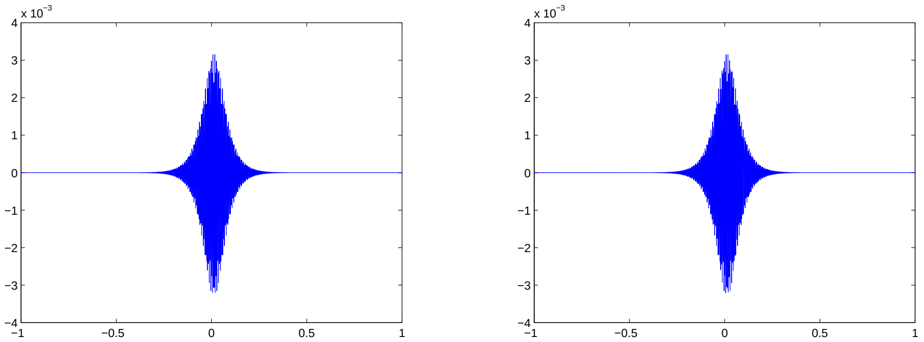

Figure 5: $\epsilon = 0.01$ and $t = 0.05$, asymptotic solution (left) and numerical solution (right).

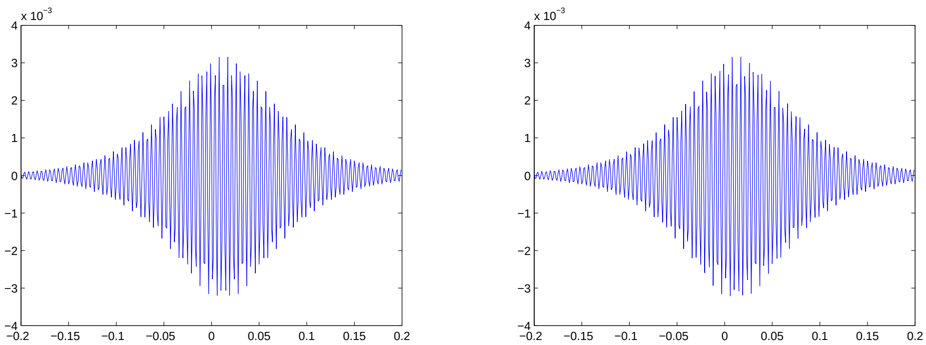

Figure 6: Continued. $\epsilon = 0.01$ and $t = 0.05$, asymptotic solution (left) and numerical solution (right).

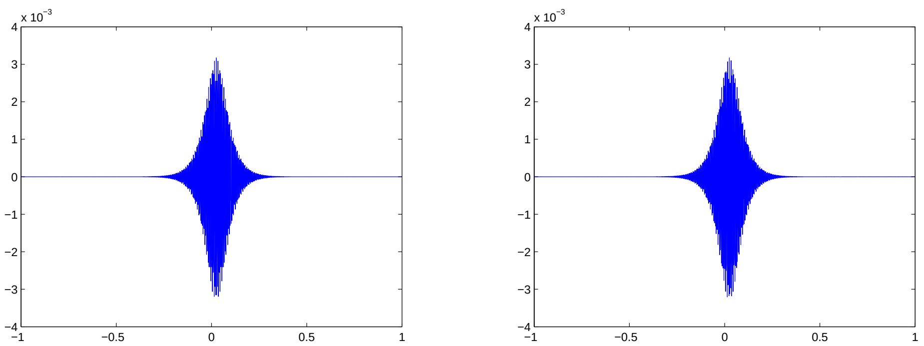

Figure 7: $\epsilon = 0.01$ and $t = 0.1$, asymptotic solution (left) and numerical solution (right).

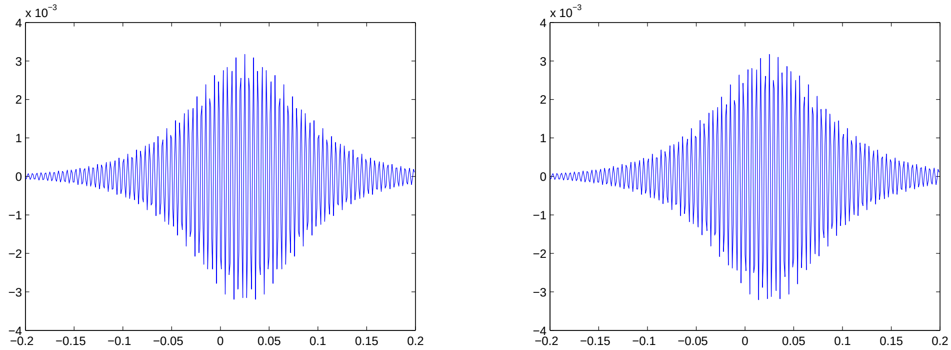

Figure 8: Continued. $\epsilon = 0.01$ and $t = 0.1$, asymptotic solution (left) and numerical solution (right).

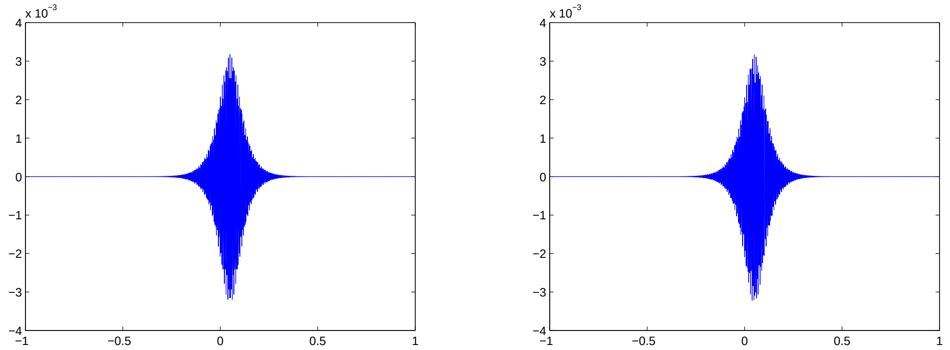

Figure 9: $\epsilon = 0.01$ and $t = 0.2$, asymptotic solution (left) and numerical solution (right).

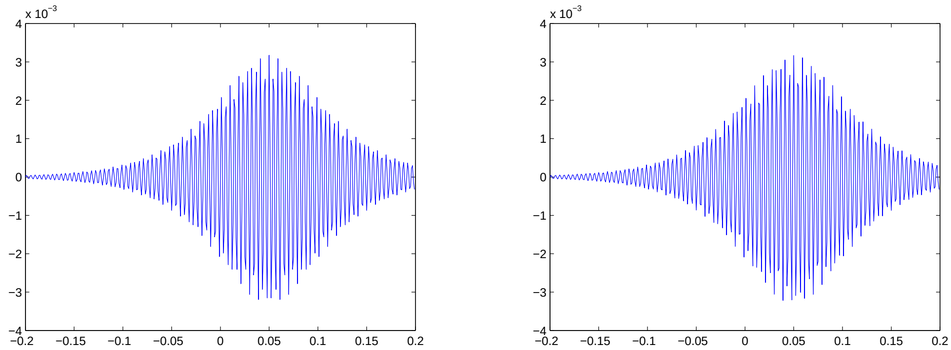

Figure 10: Continued. $\epsilon = 0.01$ and $t = 0.2$, asymptotic solution (left) and numerical solution (right).

8 and 10). We notice that the solutions to (5.9) exhibit highly oscillatory behaviors which are extremely difficult to compute but are well captured by the MSFP method. Fig. 11 shows the errors in discrete global energy and momentum.

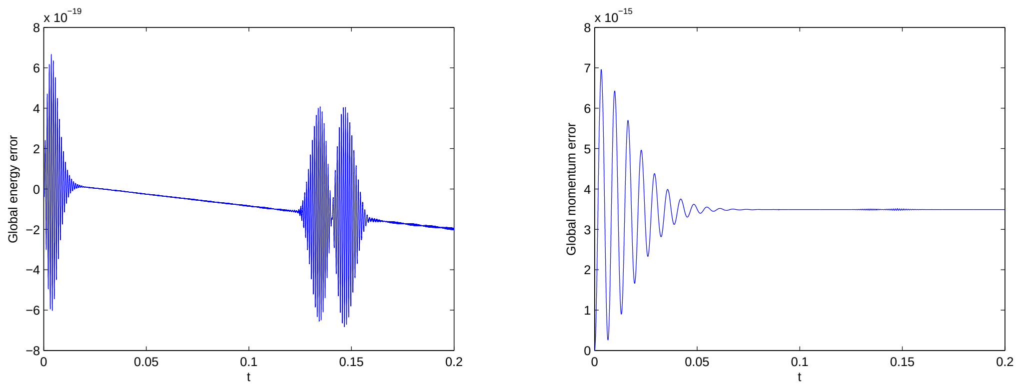

Figure 11: Global energy errors (left) and global momentum errors (right).

6 Conclusions

We propose a MSFP method for the Kawahara equation with periodic boundary condition and derive the relationship between the SDM and DFT. By using the FFT algorithm in numerical experiments, we save a lot of storage space and a large amount of calculations. Numerical experiments show that the MSFP method for the Kawahara equation is very effective. We also note that highly oscillatory behaviors can be captured well.

Acknowledgments

This work is supported by the Jiangsu Collaborative Innovation Center for Climate Change, the National Natural Science Foundation of China (Grant Nos. 11271195, 41231173 and 11201169) and Qinglan Project of Jiangsu Province of China.

References

[1] T.J. Bridges and G. Derks, Linear instability of solitary wave solution of the Kawahara equation and its generalizations, SIAM J. Math. Anal., 33(2002), 1356-1378.
[2] R. Kawahara, Oscillatory solitary waves in dispersive media, J. Phys. Soc. Japan, 33(1972), 260-264.
[3] P.J. Olver, Hamiltonian perturbation theory and water waves, Contemp. Math., 28(1984), 231-249.
[4] W. Craig and M.D. Groves, Hamiltonian long-wave approximations to the water-wave problem, Wave Motion, 19(1994), 367-389.
[5] S.P. Tao, S.B. Cui, Existence and uniqueness of solutions to nonlinear Kawahara equations, Chin. Ann. Math. Ser. A, 23(2002), 221-228.
[6] J.M. Yuan, J. Shen and J.H. Wu, A Dual-Petrov-Garlerkin method for the Kawahara-type equation, J. Sci. Comput., 34(2008), 48-63.

[7] W.P. Hu and Z.C. Deng, Multi-symplectic method for generalized fifth-order KdV equation, Chin. Phys. B, 17(2008), 3923-3929.

[8] T.J. Bridges, Multi-symplectic structures and wave propagation, Math. Proc. Camb. Phil. Soc., 121(1997), 147-190.

[9] T.J. Bridges and S. Reich, Multi-symplectic Integrators: numerical schemes for Hamiltonian PDEs that conserve symplecticity, Phys. Lett. A, 284(2001), 184-193.

[10] S. Reich, Multi-symplectic Runge-Kutta collocation methods for Hamiltonian wave equations, J. Comput. Phys., 157(2000), 473-499.

[11] T.J. Bridges and S. Reich, Numerical methods for Hamiltonian PDEs, J. Phys. A: Math. Gen., 39(2006), 5287-5320.

[12] T.J. Bridges and S. Reich, Multi-symplectic spectral discretizations for the Zakharov-Kuznetsov and shallow water equations, Phys. D, 152-153(2001), 491-504.

[13] J.B. Chen and M.Z. Qin, Multi-symplectic Fourier pseudospectral method for the nonlinear Schrödinger equation, Electr. Trans. Numer. Anal, 12(2001), 193-204.

[14] Y.M. Chen, S.H. Song and H.J. Zhu, Multi-symplectic methods for the Ito-type coupled KdV equation, Appl. Math. Comput., 218(2012), 5552-5561.

[15] H.J. Zhu, S.H. Song and Y.M. Chen, Multi-symplectic wavelet collocation method for Maxwell's equations, Appl. Math. Mech., 3(2011), 663-688.

[16] B. Moore and S. Reich, Backward error analysis for multi-symplectic integration methods, Numer. Math., 95(2003), 625-652.

[17] Y.S. Wang, B. Wang and X. Chen, Multisymplectic Euler box scheme for the KdV equation, Chin. Phys. Lett., 24(2007), 312-314.

[18] Y. Chen, Y.J. Sun and Y.F. Tang, Energy-preserving numerical methods for LandauCLifshitz equation, J. Phys. A: Math. Theor., 44(29)(2011):295207.

[19] J.X. Cai, A multisymplectic explicit scheme for the modified regularized long-wave equation, J. Comput. Appl. Math., 234(2010), 899-905.

[20] B.N. Ryland, B.I. McLachlan and J. Frank, On multisymplecticity of partitioned Runge-Kutta and splitting methods, Int. J. Comput. Math., 84(2007), 847-869.

[21] L.H. Kong, J.L. Hong and J.J. Zang, Splitting multi-symplectic integrators for Maxwell's equation, J. Comput. Phys., 229(2010), 4259-4278.

[22] L.H. Kong, J.J. Zhang, Y. Cao, Y.L. Duan and H. Huang, Semi-explicit symplectic partitioned Runge-Kutta Fourier pseudo-spectral scheme for Klein-Gordon-Schrödinger equations, Comput. Phys.Commun., 181(2010), 1369-1377.

[23] J. Wang, A note on multi-symplectic fourier pseudospectral discretization for the nonlinear Schrödinger equation, Appl. Math. Comput., 191(2007), 31-41.

[24] J.B. Chen, Symplectic And Multisymplectic Fourier Pseudospectral Discretizations for the Klein-Gordon Equation, Lett. Math. Phys., 75(2006), 293-305.

[25] Z.Q. Lv, M. Xue, and Y.S. Wang, A new multi-symplectic scheme for the KdV equation, Chin. Phys. Lett., 28(6)(2011):060205.

[26] T.B. Benjamin, The stability of solitary waves, Proc. Roy. Soc. London A, 23(1972), 153-183.